HHS Public Access

Author manuscript

Int J Min Sci Technol. Author manuscript; available in PMC 2017 August 01.

Published in final edited form as:

Int J Min Sci Technol. 2017 January ; 27(1): 91–99. doi:10.1016/j.ijmst.2016.10.003.

Analysis of the design and performance characteristics of pumpable roof supports

Batchler Timothy*

NIOSH, Office of Mine Safety and Health Research, Pittsburgh, PA 15236, USA

Abstract

Pumpable roof supports are currently being used to provide a safe working environment for longwall mining. Because different pumpable supports are visually similar and installed fundamentally in the same manner as other supports, there is a tendency to believe they all perform the same way. However, there are several design parameters that can affect their performance, including the cementitious material properties and the bag construction practices that influence the degree of confinement provided. A full understanding of the impact of these design parameters is necessary to optimize the support application and to provide a foundation for making further improvements in the support performance. This paper evaluates the impact of various support design parameters by examining full-scale performance tests conducted using the National Institute for Occupational Safety and Health (NIOSH) Mine Roof Simulator (MRS) as part of manufacturers' developmental and quality control testing. These tests were analyzed to identify correlations between the support design parameters and the resulting performance. Based on more than 160 tests over 7 years, quantifiable patterns were examined to assess the correlation between the support dimensions, cementitious material type, wire pitch, and single-wall vs. dual-walled bag designs to the support capacity, stiffness, load shedding events, and yield characteristics.

Keywords

Pumpable; Roof support; Performance characteristics; Secondary support

1. Introduction

Developed in the 1990s, the first major use of pumpable supports systems in U.S. longwall operations was in the support of bleeder entries [1]. Since then, they have been utilized as yieldable concrete supports to provide a safe working environment for longwall mining gateroads, bleeders, and emergency escapeways while also maintaining adequate ventilation pathways. The basic structure of pumpable roof supports has remained unchanged over the years. Formed in place with a two-part fast-setting grout, the support material can be pumped into a containment bag from several thousand feet away, often through surface boreholes. The containment bag then acts as a form to fill the support and provides confinement to the grout during loading and after failure. Pumpable roof supports provide

*Tel.: +1 412 3866844. tbatchler@cdc.gov.

full contact with the mine roof and floor, which eliminates the need for secondary material to establish proper roof contact (see Fig. 1). They provide a high peak load capacity and a sustained, confinement-controlled yield behavior while maintaining stable ground conditions, which is essential to underground mining operations.

Over the years, considerable research has been conducted to develop pumpable support technologies and to evaluate their performance characteristics to improve the support design. Performance traits, installation patterns, and ground control observations in various geological and mining conditions were evaluated to determine the support performance characteristics and correlation to observed ground responses [2–4]. To examine performance, the load displacement characteristics of the pumpable roof support can be determined from full-scale testing conducted using the National Institute for Occupational Safety and Health (NIOSH) Mine Roof Simulator (MRS) located in Bruceton, PA [1].

Because pumpable supports all look similar, the tendency is to think that they all perform the same. However, several design parameters can affect the performance characteristics of the pumpable support system. This paper evaluates the impact of various support design parameters by examining full-scale performance tests conducted at the NIOSH MRS as part of various product development and quality control testing. These tests were analyzed to identify correlations between the support design parameters and the resulting performance. Based on more than 160 tests over 7 years, quantifiable patterns were examined to assess the correlation of the support dimensions, cementitious material type, wire pitch, and single-wall vs. dual-walled bag designs to the support capacity, stiffness, load shedding events, and yield characteristics.

2. Design features

For many years, pumpable roof supports have been installed in mines to support the roof. The supports are designed to be installed in place using a pumpable cementitious grout. Typically, a two-component material is pumped from a surface installation through an access borehole into a containment bag to form the support, with the capability to pump the material a distance of over 5486 m [3]. The unfilled support bags are transported into the mine in a collapsed configuration, minimizing the transportation needs to the installation site. During installation, the bags are secured to the mine roof and then extended down to the floor. The solidified grout material captured by the containment bag provides a full support column between the mine roof and floor without the need for any additional materials, providing a significant advantage over most other support designs.

Pumpable roof support systems have evolved during the last 20 years, with improvements made to the bag design and several variations of cementitious materials in an effort to optimize cost and performance. Currently, there are two basic types of material used: calcium-sulfo-aluminate (CSA) and Portland-based cementitious grouts. The CSA grout contains no Portland material and generally has an inherently faster setup time and strength gain than Portland grouts without the use of accelerating additives. Both materials are pumped in separate two-part mixes such that the reactive chemistry only occurs once the materials are mixed together just prior to entering the support bag. One interesting physical

difference between the two materials is that some samples of the Portland-based materials severely decompose (lose structural integrity) when exposed to air, while the CSA grout once cured is insensitive to air and does not physically deteriorate. The primary performance difference is that the supports made with the higher-modulus CSA material achieve peak compressive strength with less displacement, providing increased support stiffness compared to the supports constructed from Portland-based material.

Temperature can play a significant role in the support installation process. Most grouts are temperature-sensitive in terms of the reactive chemistry, which affects both the setup time and the material strength when the water temperature used to make the grout slurries falls beyond the required specifications. Typically, a water heater at the surface pumping station is used to ensure the water is the proper temperature in colder weather. Depending on the setup time, supports are often filled in several lifts. If the grout does not set up fast enough, the bag will tend to bow outward from the roof to the floor, potentially degrading the capacity of the support by as much as 10% [1].

A high loading stiffness with a sustainable residual load through several centimeters of convergence is one of the universal design features of pumpable supports. The high loading stiffness causes the support to reach a peak load capacity within a short amount of convergence. For a passive roof support, this is beneficial to roof control as the support resistance is mobilized quickly to work to control the roof deformation. The peak load is typically followed by a sequence of load shedding events, which results in sharp drops in load. These sudden drops in load are caused by the brittle grout fracturing induced from the stress of convergence. The subsequent residual load behavior is dependent on the confinement and integrity of the support bag. A full understanding of the impact of these design features is necessary to optimize the support applications and to provide a foundation for making improvements in the support performance.

3. Performance characteristics

The performance characteristics for pumpable roof support entail four main factors, as illustrated in Fig. 2, namely stiffness, peak load capacity, load shedding events, and residual load characteristics.

Stiffness is defined as the resistance offered by an elastic body to deformation. The pumpable support loading stiffness is calculated using the linear portion of the loading cycle prior to grout failure and load shedding events (see Fig. 2). It measures the capacity of the support to develop load as a function of convergence. Stiffness is important in designing supports since, as passive supports, the load resistance is only developed through convergence of the mine opening, and excessive convergence leads to unstable ground conditions. Therefore, high load stiffness is desirable.

Peak load capacity is the maximum capacity of the support and is often referred to as the support strength. The compressive strength of the cementitious grout and the confinement pressure provided by the pumpable support bag control the peak load capacity. When the

compressive strength of the grout is exceeded, the grout will fracture and the support will abruptly shed some of its load capacity.

As with most structures made from brittle material, failure is associated with a major drop in load once the compressive and shear strength of the material are exceeded. This is common in all pumpable supports. As illustrated in Fig. 2, the support quickly recovers from the initial load shedding event, restoring a loading stiffness that is very close to the pre-failure loading stiffness. It is believed that the restoration of the support stiffness following a load shedding event is attributed to reestablishment of confining pressure caused by the dilation of the support body and resistance provided by the bag and wire wrap system. As shown in Fig. 2, this restoration of confinement and subsequent loading stiffness may be sufficient to allow continued development of load capacity. The peak load capacity occurs when this confining pressure can no longer be fully restored. The load shed associated with the peak load is generally, but not always, the largest of the set. As illustrated in Fig. 2, the restoration loading stiffness following the peak load shedding event is reduced. The residual load will vary depending on the severity of the grout fracturing and the capability of the bag and wire to maintain confining pressure.

A progressive failure behavior occurs through a series of subsequent load shedding events following the peak loading. The continued bulking of the fractured grout material stretches the bag and wire wrap, resulting in a tendency of continued decreased stiffness during load restoration following the load shed events (Fig. 2). A load shed event is defined as a sudden drop of load capacity of over 222 kN within less than 0.76 cm of displacement. This action of successive load shedding and declining load restoration continues until the wire breaks, which generally occurs after several centimeters of convergence. Once the wire breaks, the bag will generally rip open, causing spillage of material out of the bag containment system and culminating in a more severe load shedding with little and often no increase in load following the event. The residual loading beyond this point depends on the severity of damage to the bag and wire containment system. The support often can provide a useful sustained loading through a few more centimeters of convergence once the wire is broken, but the capacity of the support is definitely compromised and less reliable that it was prior to the wire breaking event.

4. Design parameters

There are several design parameters that affect the performance characteristics of the pumpable support system. Based on more than 160 full-scale tests of various pumpable supports in the NIOSH MRS as part of various vendor developmental and quality control testing, quantifiable patterns were examined to assess the impact of the following design parameters: (1) cementitious material type, (2) support dimensions, (3) wire pitch, and (4) single-wall vs. dual-wall bag construction. It is important to note that a controlled experimental plan was not executed, and as such there is some potential for performance bias based on the variability in support designs included in the study population.

4.1. Cementitious material type

There is a strong relationship between the support performance and the cementitious material used for the support construction. Two different cementitious grouts (CSA and Portland) were evaluated in this study. Fig. 3 shows the mean and standard deviation of peak load capacities for supports constructed from the two cementitious grouts, along with the mean and standard deviation of the convergence at peak load capacity. In general, the peak load capacity of the CSA supports was higher than for the equivalent Portland supports. The mean peak load capacity of a standard 76-cm-diameter support with a 10-cm wire containment bag constructed from CSA material was 2389 kN. This compares to the mean peak load of the Portland-based material supports of 1735 kN. Therefore, for a 76 cm-diameter support, the CSA support provided about 38% more capacity than the Portland-based support. However, this magnitude of higher load capacity for CSA was not consistent for all the support sizes. The CSA material provided only 17% more capacity than the Portland-based material for the 69 cm-diameter and 76 cm-diameter supports. Conversely, the Portland material provided 10% more capacity than the CSA material for the 61 cm-diameter support. The likely reason for the higher peak load capacity for the 61-cm Portland supports was an increase in confinement of the bag system due to a closer wire wrapping around the support circumference. These tests provide some insight into the impact of the different cementitious materials on the peak load capacity of pumpable supports.

The pre-peak loading stiffness of the supports constructed from the CSA material was consistently higher than for the Portland material for all support sizes as documented in Table 1. Fig. 3 shows the mean and standard deviation of the convergence at peak load for each of the cementitious type pumpable roof supports. The supports constructed with CSA material exhibited a higher stiffness that resulted in the peak load being reached at much less displacement. The CSA supports reached peak loading between 1.5 and 2.8 cm of convergence compared between 6.3 and 6.9 cm for the Portland supports to reach peak loading.

Load shed events are sudden drops in support load capacity as the grout fractures from the induced stress from convergence. A major load shed event is defined as a sudden drop of load capacity of over 222 kN within less than 0.76 cm of displacement. Fig. 4 illustrates the number of load shed events generated prior to the peak load capacity for the CSA-based and Portland-based supports. These values represent the distribution of the percentage of the number of load shed events during a full-scale test using the full complement of tests available in this study. By far, the most common behavior is no load shed events prior to the peak loading. Since the peak loading is controlled by the grout strength, this would be the expected behavior. The lower occurrences of CSA load sheds prior to peak load could be attributed to the fact that the convergence at peak load capacity for CSA based material was 1.5–2.8 cm compared to 6.4–6.9 cm for the Portland-based material. The lower stiffness of the Portland-based supports gives more opportunity for a grout fracture to occur, resulting in a load shedding event.

Fig. 5 shows the distribution of the number of load shed events that occurred during a loading cycle following the peak load capacity and through 15.25 cm of convergence for the two cementitious grouts. It was rare for the CSA supports to exhibit no load shedding events

following peak loading (5%). Conversely, Portland supports exhibited no load shedding events 24% of the time. The most common number of load sheds for the Portland supports was one, which occurred 41% of the time, compared to the CSA material, which had two load shed events occurring 25% of the time. Similar to the trend showing fewer load sheds prior to peak load capacity, the higher number of load sheds for the CSA material could be attributed to the fact that the peak load capacity was achieved at a lesser displacement.

Fig. 6 shows the distribution of the number of load shed events (percentage) within the first 15.25 cm of convergence for both cementitious grouts. The highest percentage of load shed events for both materials was three. The Portland-based supports experienced three load shed events for 28% of the tests, and the CSA-based supports experienced three load shed events for 25% of the tests. The most common distribution of the number of load shed events was 1–3 for the Portland-based supports and 2–5 for the CSA-based supports. Overall, more load shed events occurred with the CSA-based supports than the Portland-based supports, suggesting that the CSA material tends to be more brittle than the Portland material.

One of the design features for a pumpable support system is to maintain a useful residual load carry capacity through several centimeters of convergence. Fig. 7 shows the representative average loading performance through 18 cm of convergence for a 76 cm-diameter CSA and Portland support with a 10-cm wire pitch construction in the support bag. The curve shows that the support load averaged over each 2.54 cm of displacement. For example, the average load for a CSA support between 11 and 14 cm was 1334 kN (see Fig. 7). This averaging process essentially diminishes the load shed events. These average performance curves are developed from the average load displacement response of 11 tests for the CSA curve and 9 tests for the Portland curve. Both support loading performances are characterized by an initial rapid increase in load capacity, indicating high stiffness, followed by an extended residual load. The average residual load for the CSA-based supports was 1334 kN compared to 1001 kN for the Portland-based supports. This pattern showed a higher residual load for CSA supports, but this trend was not consistent with all the support design variations. The average residual load for Portland supports was higher by as much as 24% for both the 69 cm-diameter and 76 cm-diameter supports with a 15 cm wire pitch. This response is inconsistent with the established trends above and is likely the result of an insufficient number of direct comparison tests of grout materials and bag construction types.

Pumpable supports are often used in higher convergence environments where an extended residual load is required. Fig. 8 illustrates the representative average loading performance for a 76 cm-diameter CSA support with a 15-cm wire pitch construction in the support bag through 30 cm of convergence. The residual load capacity is highly dependent on the confinement provided by the containment bag and functions until the bag is severely damaged and the crib material starts to fall out. A well-designed pumpable support will generally maintain a fairly high residual load through about 25 cm of displacement as seen in Fig. 8.

4.2. Support dimensions

The support dimension controls several factors including peak capacity, stiffness, and residual loading. Theoretically, the peak capacity and stiffness should be directly proportional to the support area, while stiffness should be inversely proportional to the support height. The area relationships were evaluated, but there were not enough height test variances to enable a proper assessment of the impact of the support height. There is no simple theoretical relationship to examine residual loading behavior relative to support area or height, but the hypothesis is that higher peak loading will result in higher residual loading as well. This hypothesis is examined from the full-scale support testing.

When using a specific cementitious grout with a consistent elastic modulus and compressive strength, the peak load capacity and stiffness should be directly related to the support area. Four different diameters of pumpable roof supports were evaluated in this study. Fig. 9 shows the mean peak load capacities of 61, 69, 76, and 91 cm-diameter pumpable roof supports. Fig. 9 illustrates the linear relationship of capacity increase with support diameter, and also shows an increase in peak load capacity of 69% for the 91 cm-diameter support compared to a 61-cm-diameter Portland support with a 10-cm wire pitch. The 7 cm wire pitch performance for the Portland supports was the least consistent in terms of the linear relationship between peak capacity and support diameter. This inconsistency is most likely driven by the limited number of tests (2–3) for each support diameter in this test configuration.

The loading stiffness of the pumpable roof supports is also proportionally related to the diameter of the pumpable roof support. For example, an increase of 61% in loading stiffness was observed when comparing a 91 cm-diameter Portland pumpable support with a 10-cm pitch bag construction with a 61 cm-diameter support. Fig. 10 illustrates the loading stiffness of 61, 69, 72, and 91 cm-diameter supports. The Portland 7 and 10 cm wire pitch had some inconsistency again due to the limited number of tests, but overall a reasonable linear relationship was observed for all test configurations. The graph also shows that the wire pitch can strongly influence the support stiffness. The impact of the wire design will be discussed later in the paper. The slopes of the stiffness lines are similar for all support configurations with the exception of the 15 cm wire pitch for the CSA supports, which had a steeper slope indicating there was an elevated increase in capacity due to the support diameter for the larger diameter supports in this configuration.

The impact of support area on load shedding prior to the support reaching peak loading is shown in Figs. 11 and 12 for diameters of 61, 69, 76, and 91 cm. Overall, the occurrence of load shed events prior to peak loading is minimal. CSA supports tended to have more load shed events prior to peak loading for the larger-diameter (76 and 91 cm) supports, while Portland-based supports tended to have more load shedding events prior to peak loading for smaller-diameter (61 and 69 cm) supports.

Figs. 13 and 14 document the number of load shed events after the peak load capacity for the 61, 69, 76, and 91 cm diameter supports. Similar to the pre-peak load capacity trend for load sheds, the CSA supports tended to have more load sheds after the peak load capacity occurred for the larger-diameter supports. The most common of load sheds was 1–3 for the

smaller-diameter supports (61 and 69 cm) and 2–5 for the two larger-diameter supports (76 and 91 cm). The Portland supports tended to have 0–2 load shed events after peak load capacity occurred.

There is some correlation between the support diameter and the residual loading of the support. As hypothesized, residual loading tended to be greater for the larger-diameter supports. An example is shown in Fig. 15, which compares the relationship for Portland supports with a 10 cm wire pitch construction in the support bag. The curve shows that the support load averaged 2.54 cm of displacement over each. For example, the average load for a 61 cm-diameter support between 11 and 14 cm was 725 kN (see Fig. 15). The average residual load between 10 and 23 cm of displacement was also compared. The average residual load for the 61 cm-diameter support was 641 kN compared to 1205 kN for the 91 cm-diameter support. This trend was also consistent with the CSA supports.

4.2.1. Wire pitch—Confinement plays a significant role in support performance, influencing both the peak load and residual load behavior. The bag is used as a form to fill the support in place underground and integrates a spiraled wire, as shown in Fig. 16, around the support to increase confinement of the fill material. When the strength of the grout is exceeded, the grout bulks through successive fracturing, and as convergence continues to stretch the bag, the bulking of the fractured grout inevitably causes a tear in the bag fabric. Without the spiraled wire to contain the bulking material, the bag would not have sufficient strength to provide enough confinement to preserve the residual loading. Eventually, after enough convergence causes excessive bulking of the fractured grout segments, the wire confinement will fail and the support experiences a sudden, unrecoverable drop in load capacity (see Fig. 17).

Any confining pressure will have a positive impact on the effective grout strength and resulting support capacity. Confining pressure can be generated by the grout pumping pressure, providing the support bag can provide the necessary resistance. This “preload” confinement can add to the peak capacity of the support. One cause for the CSA support capacity being less than what would be expected from the material compressive strength is the existence of hairline pre-existing fractures. These hairline fractures may come from the expansion of the grout material during the hydration of the cement components as the grout cures and hardens in the support bag [5]. These pre-existing fractures can be seen on the surface of the support if the bag is removed, and they appear to control the fracture behavior of the grout during loading. Confining pressure will help to control the shear stress and subsequent fracture development. Fig. 18 shows results from two full-scale tests comparing the maximum support capacity with the containment bag as normal and with the containment bag removed after the support was pumped and the grout fully cured. The support peak capacity was increased by 94% by the confinement of the bag, and the residual loading without the bag was quickly lost following the load shedding after the peak capacity was obtained.

As previously indicated, confinement is largely provided by the wire wrap integrated into the support bag. One way the confinement of the support can be increased is by reducing the spacing (pitch) of the spiral wire. Fig. 19 shows the increase in support capacity of a 69 cm-

diameter Portland-based support by comparing a 7, 10, and 15 cm wire pitch. The benefit of the closer wire spacing can be seen as the performance of a bag with the 7 cm wire pitch has a 54% higher peak load capacity than the 15 cm wire pitch bag. Capacity improvements for other support configurations due to wire pitch can also be seen in Fig. 9.

Table 2 compares the average loading stiffness of the 69 cm-diameter, Portland-based supports. A 36% increase in the loading stiffness was observed with a change in the wire pitch from 15 to 10 cm for the support. A 61% increase in loading stiffness was observed when changing the wire pitch spacing from 15 to 7 cm. However, this magnitude of elevated loading stiffness was not consistent with every size of Portland-based supports. When comparing the 15 to 10 cm wire pitch for the 76 cm-diameter and 91 cm-diameter supports, the increase in loading stiffness was 26% and 3%, respectively.

4.3. Single-wall vs. dual-wall bag construction

The majority of tests evaluated (73%) used a standard single-wall, wire-wrapped (external) containment bag for the full-scale evaluation of the pumpable supports. The rest of the tests consisted of various prototype bags (11%) and dual-wall containment bags (16%). The dual-wall construction containment bag includes an internal cylindrical mesh with a spiral wire reinforcement within the bag (Fig. 20). The inner mesh is located about 4–7 cm inside the external bag. This design allows the cementitious fill material to encapsulate the mess reinforcement and fill the external bag during installation. The design goal of the dual bag is to increase the residual load capacity of the support and was used only in conjunction with CSA supports in the NIOSH tests.

The mean peak load capacities of the dual-wall support constructions were higher than the equivalent single-wall support constructions in the majority of the tests. Fig. 21 compares the peak load capacity for 76 cm-diameter supports with standard single-wall and dual-wall constructions with a wire pitch spacing of 10 and 15 cm. In this example, the mean peak load capacity of a dual-wall support with a 10 cm wire pitch was 2713. This compares to the mean peak load capacity of single-wall support of 2389. Therefore, for a 76 cm-diameter support with a 10 cm wire pitch, the dual-wall containment bag provided about 14% more capacity than the single-wall support.

The average loading stiffness of the dual-walled pumpable supports with a 10-cm wire pitch was 2718 kN/cm compared to 2317 kN/cm for the equivalent single-walled supports (Table 3). This resulted in the dual-wall supports being on average 17% stiffer than the single-wall supports. This trend was also consistent with the 15 cm wire-pitch supports, which showed a stiffness increase of 34% from a dual-wall to single-wall construction.

The 76 cm-diameter, 10 cm wire pitch CSA supports were examined to determine the effect of dual-wall vs. single-wall construction on load shedding. The dual-wall construction does not significantly affect the number of load shed events generated prior to the peak load capacity being reached, since the initial load shed events are largely controlled by the compressive and shear strength of the grout instead of the confinement. Both the single-wall and dual-wall supports experienced load shed events prior to the peak load capacity only

18% of the time. Dual-wall support constructions tended to have more load shed events post-peak loading than the single-wall containment bags (see Fig. 22).

The dual-wall supports maintained a higher residual load on average than the single-wall supports. Fig. 23 compares the representative performance between 0 and 18 cm of displacement, showing the load averaged over each 2.54 cm of displacement. The average residual load for the dual-wall supports was 1379 kN compared to 1001 kN for the single-wall supports—a 38% increase. The results further confirm that the residual load capacity is influenced by the confinement provided by the containment bag.

5. Conclusions

In this study, the stiffness of the supports constructed from CSA material was significantly higher than for the Portland material for all support sizes. Likewise, the peak load capacities of the CSA supports were mostly higher than the equivalent Portland supports.

Confinement also plays a significant role in the support performance, influencing both the peak load and residual load behavior. The bag is used as a form for filling the support in place underground and integrates a spiraled wire that wraps around the pumpable support to increase confinement of the fill material. There is a direct relationship between the wire spacing (pitch) and the capacity of the support, with increased capacity provided by the added confinement of closer wire spacing. Wire spacings of 7, 10, and 15 cm are utilized in current pumpable support constructions. The wire diameter and material properties were not evaluated in this study, but the variances in these factors among the bag constructions are believed to be relatively minor.

The failure behavior of pumpable supports, like all brittle material, occurs when the support stress exceeds the compressive and shear strength of the material, causing a load shed event. A sequence of significant load shedding events occurs during loading and the support typically fails progressively while providing a sustained residual loading through several centimeters of displacement (typically 18–25 cm) before the wire breaks. Once the wire breaks, the confinement is significantly compromised, which, in combination with the bag ripping open and grout material spilling out, causes a more rapid deterioration of useful residual loading and yielding capability. A well-designed pumpable support can provide a useful residual load through 25–41 cm of convergence.

Currently, progressive load shedding is a common and unavoidable consequence of the material used for this type of support construction. Therefore, reducing load shedding behavior with this type of support construction will have to be achieved by altering the fill materials’ properties to eliminate the brittle failure and highly bulked behavior of the failed material. NIOSH is planning to conduct additional studies that evaluate other less brittle and more crushable materials to determine the feasibility of reducing load shedding with the current containment bag constructions.

References

1. Barczak TM, Tadolini SC. Pumpable roof supports: an evolution in longwall roof support technology. Transactions of the Society for Mining, Metallurgy, and Exploration, Inc. 324:19–31.
2. Dolinar, D. Ground and standing support interaction in tailgates of western U.S. longwall mines used in the development of a design methodology based on the ground reaction curve. Proceedings of 22nd international conference on ground control in mining; West Virginia University. 2010. p. 152-60.
3. Campoli, AA. Selection of pumpable cribs for longwall gate and bleeders entries. Procedures of 34th international conference on ground control in mining; West Virginia University. 2015. p. 80-2.
4. Zhang, P., Milam, M., Mishra, M., Hudak, WJ., Kimutis, R. Requirements and performance of pumpable cribs in longwall tailgate entries and bleeders. Proceedings of 31st international conference on ground control in mining; West Virginia University. 2012. p. 1-11.
5. Barczak, TM., Chen, J., Bower, J. Pumpable roof supports: developing design criteria by measurement of the ground reaction curve. Proceedings of 22nd international conference on ground control in mining; West Virginia University. 2003. p. 283-93.

Fig. 1.
Pumpable roof supports in a longwall recovery room.

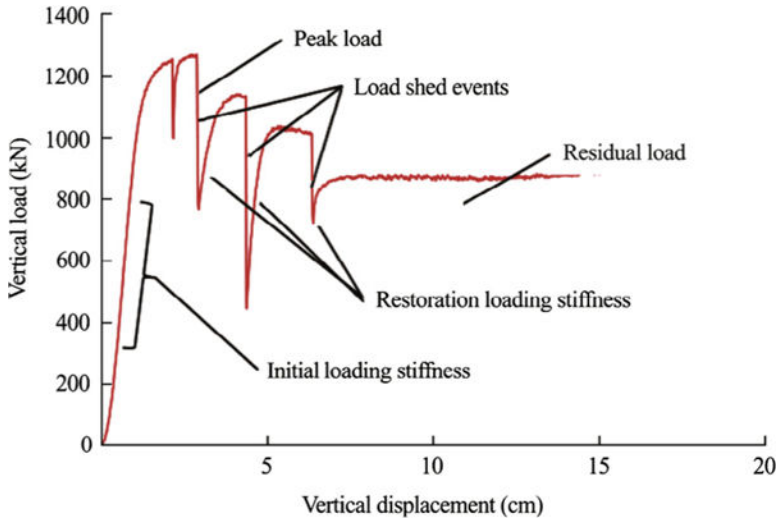

Fig. 2.
Illustration of performance characteristics for a pumpable roof support loading profile.

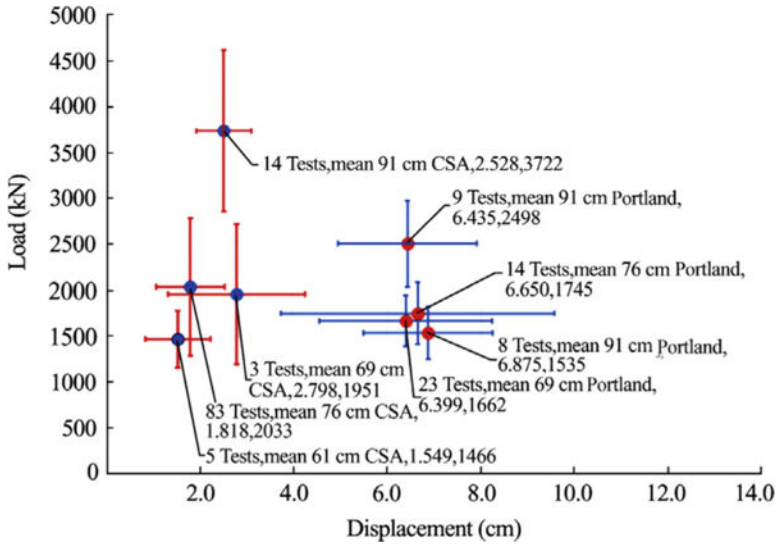

Fig. 3.

Comparison of the peak loading capacity of the CSA and Portland-based supports.

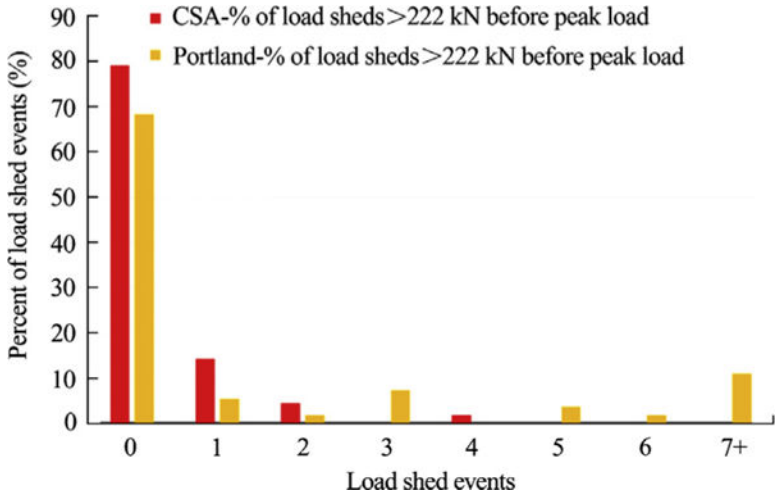

Fig. 4.

Distribution of the percentage of the number of load sheds occurring prior to the peak load capacity for CSA and Portland-based supports.

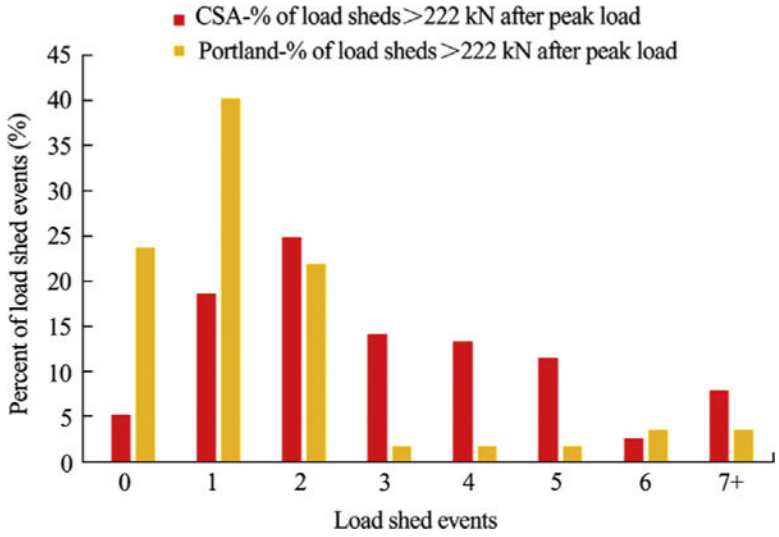

Fig. 5.

Distribution of the percentage of the number of load sheds occurring after the peak load capacity for CSA and Portland-based supports.

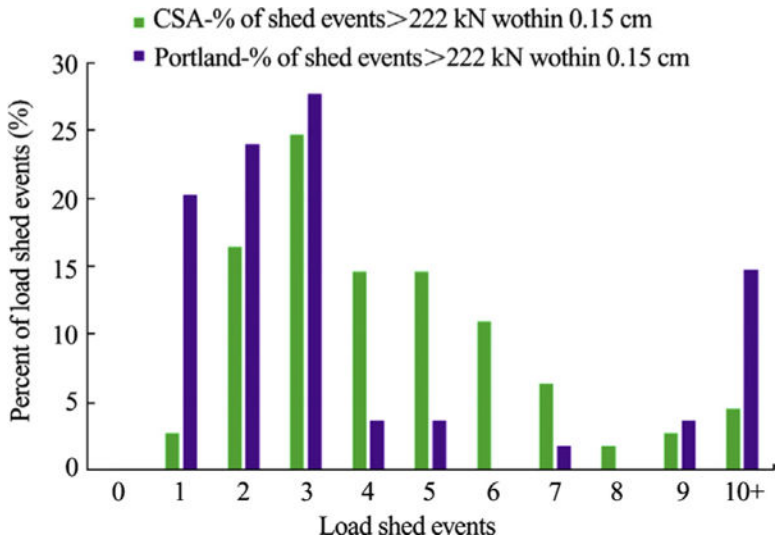

Fig. 6.

Distribution of the percentage of the number of load sheds occurring from 0 to 15.25 cm of displacement for CSA and Portland-based supports.

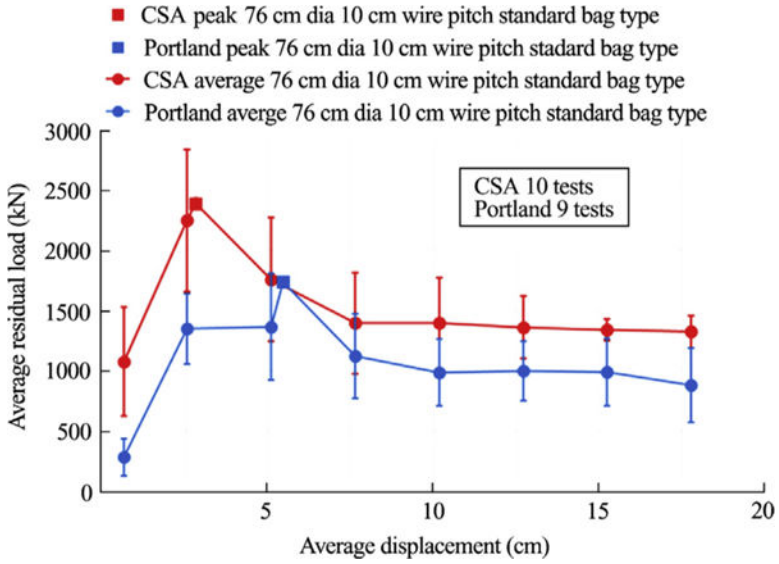

Fig. 7.

Representative average loading performance for a 76 cm-diameter CSA and Portland support.

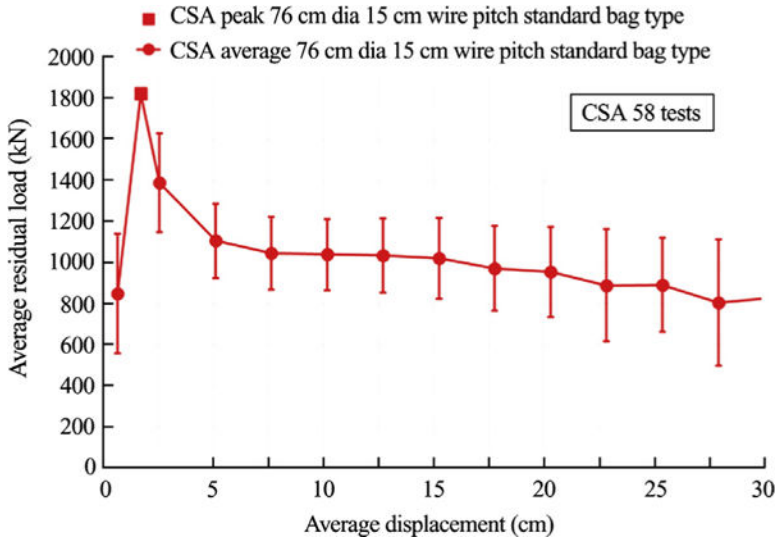

Fig. 8.

Representative average loading performance for a 76 cm-diameter CSA support through 30 cm of displacement.

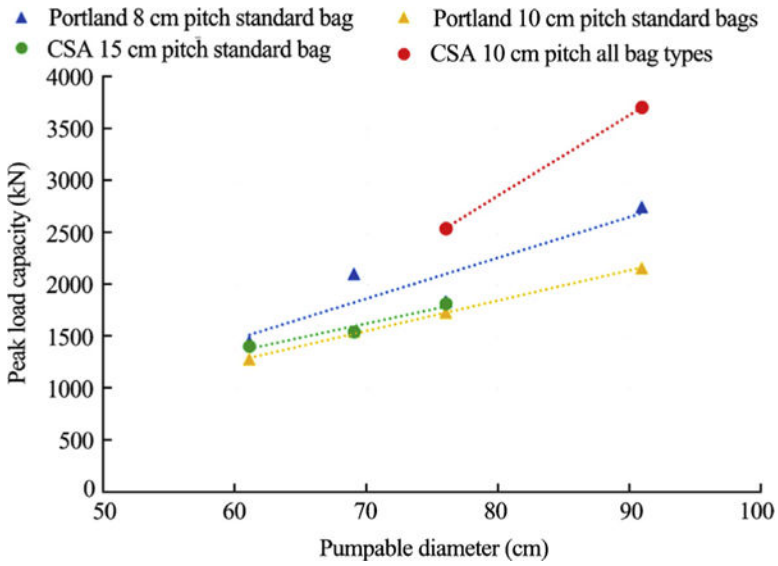

Fig. 9.

Trend showing increase in peak load capacity in relationship to the support diameter.

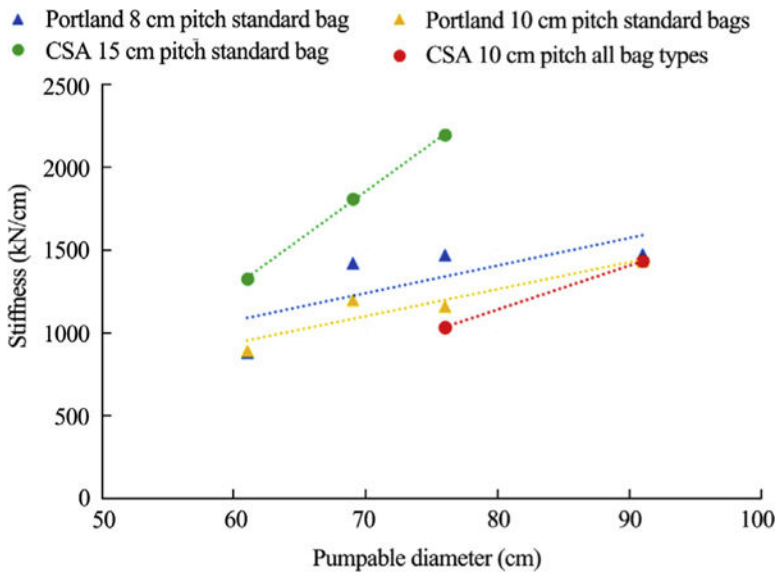

Fig. 10.
Trend showing increase in stiffness in relationship to the support diameter.

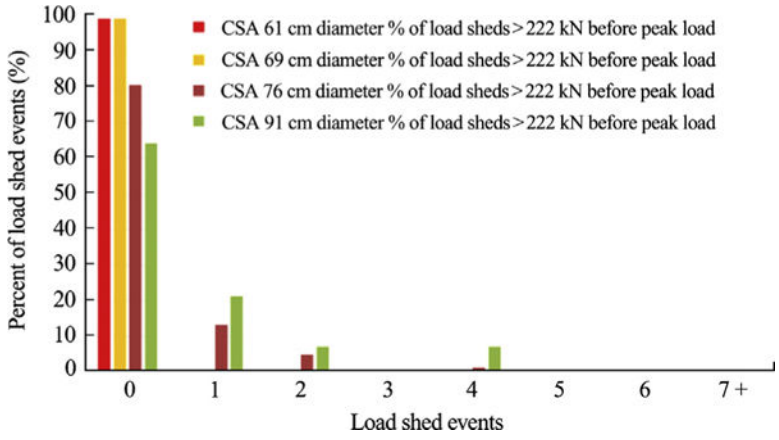

Fig. 11.

Distribution of the percentage of the number of load sheds occurring prior to the peak load capacity for 61, 69, 76, and 91 cm diameter CSA pumpable roof supports.

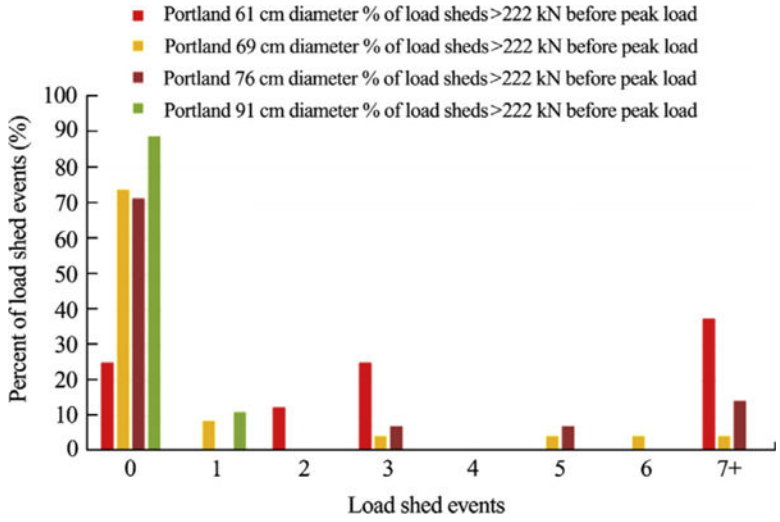

Fig. 12.

Distribution of the percentage of the number of load sheds occurring prior to the peak load capacity for 61, 69, 76, and 91 cm diameter Portland pumpable roof supports.

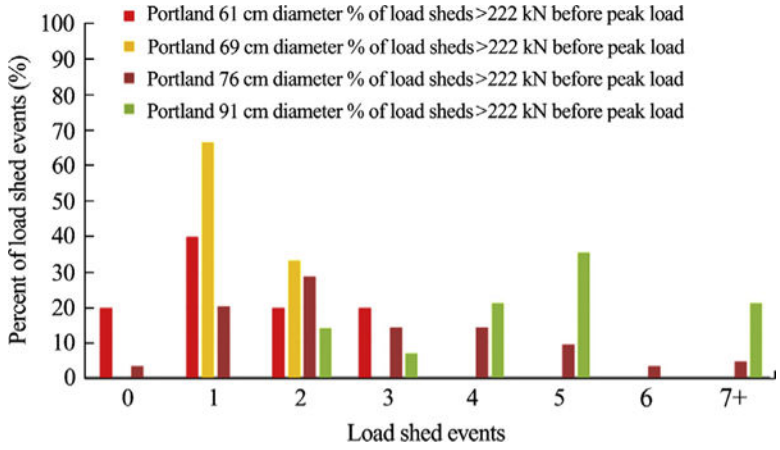

Fig. 13.

Distribution of the percentage of the number of load sheds occurring after the peak load capacity for 61, 69, 76, and 91 cm-diameter CSA pumpable roof supports.

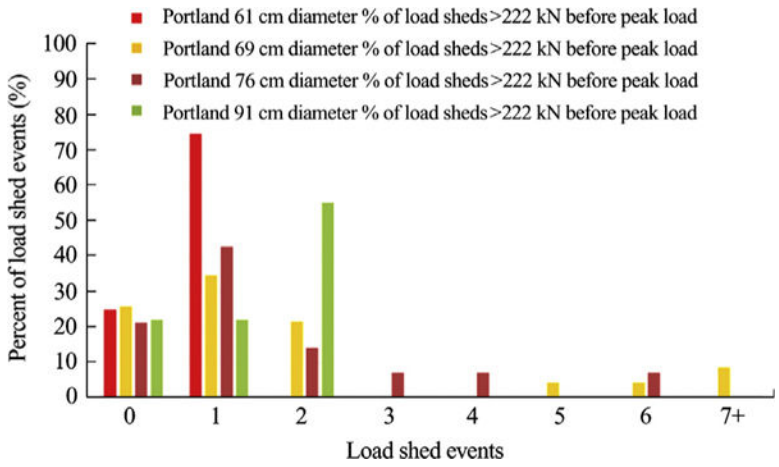

Fig. 14.

Distribution of the percentage of the number of load sheds occurring after the peak load capacity for 61, 69, 76, and 91 cm-diameter Portland pumpable roof supports.

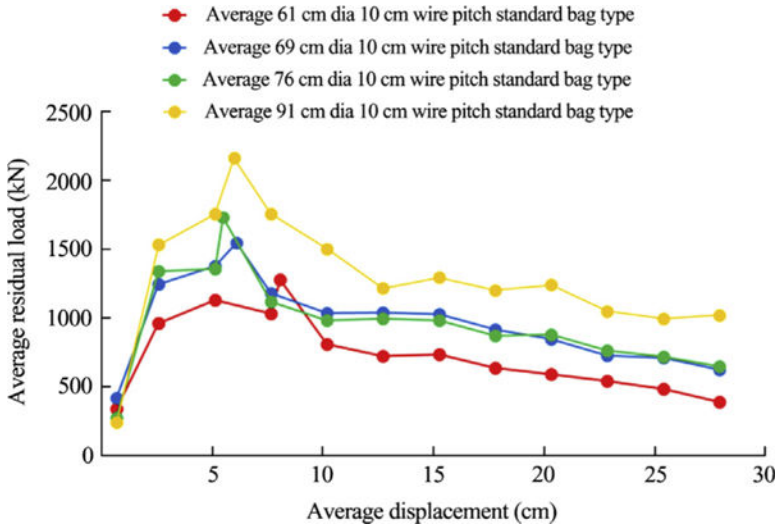

Fig. 15.

Representative average loading performance for 61, 69, 76, and 91 cm-diameter Portland pumpable roof support.

Fig. 16.
Containment bag seam securing a metal reinforcement wire that is spiraled from the top to the bottom of the bag.

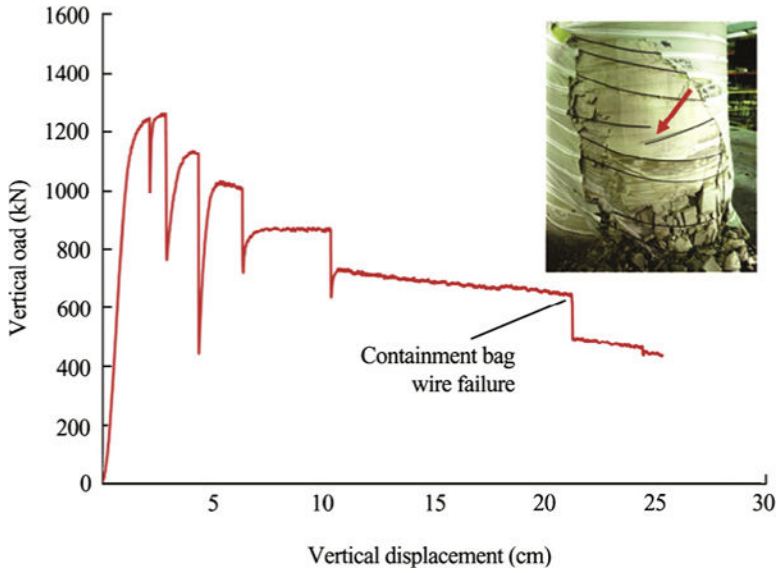

Fig. 17.
Failure of the wire confinement within the pumpable containment bag.

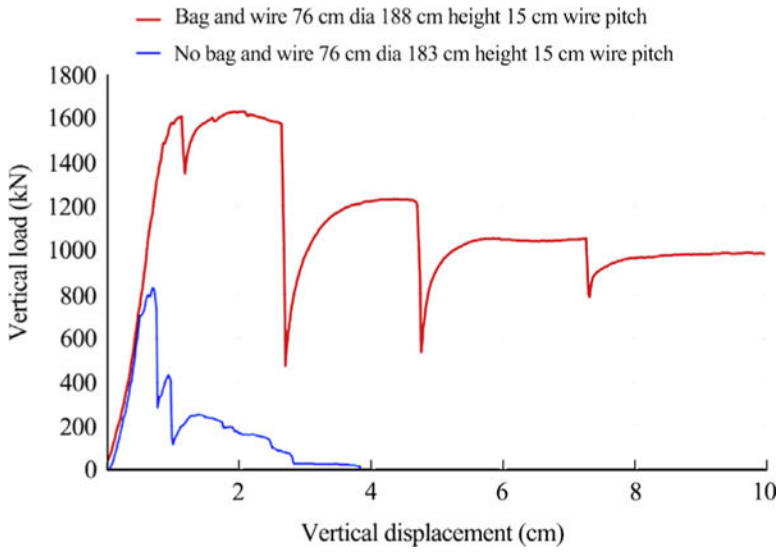

Fig. 18.

Comparison of support capacity with and without the containment bag.

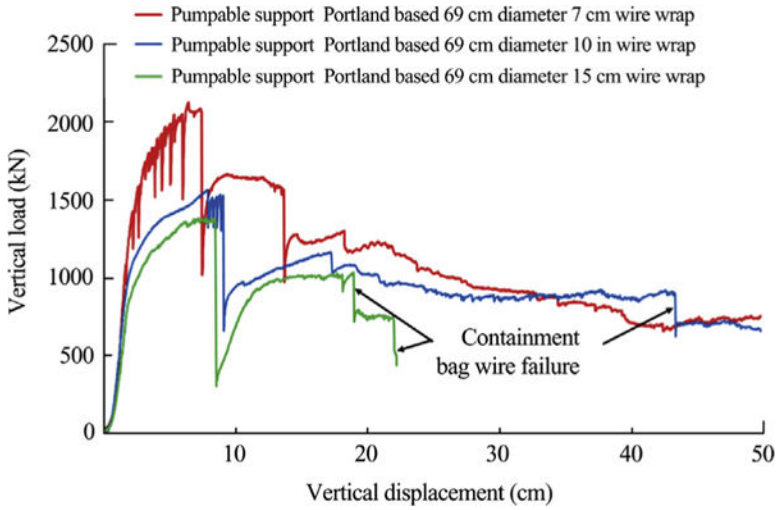

Fig. 19.

Performance comparison displaying the increased load capacity due to increased confinement from closer wire spacing.

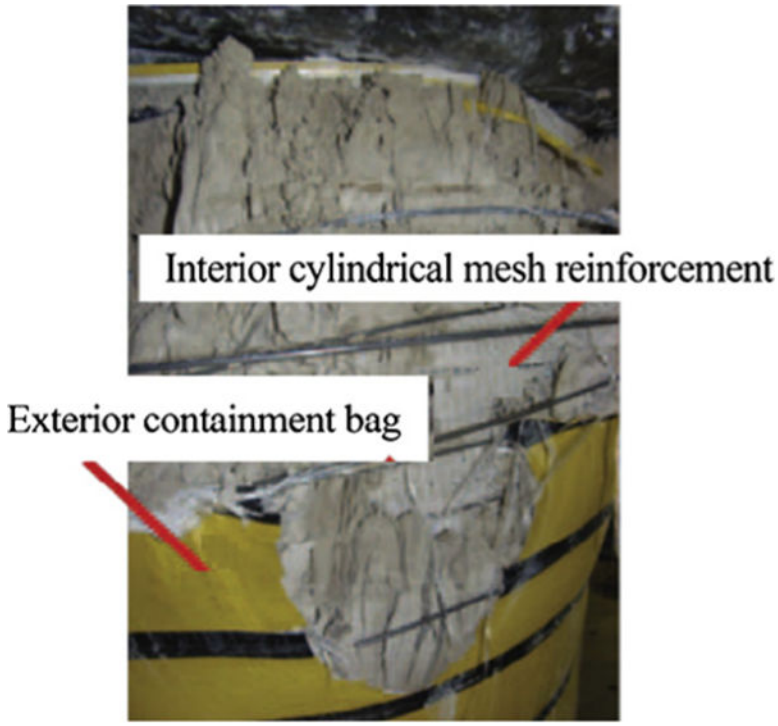

Fig. 20.
Bag construction showing inner mesh that ripped open during performance testing in NIOSH Mine Roof Simulator.

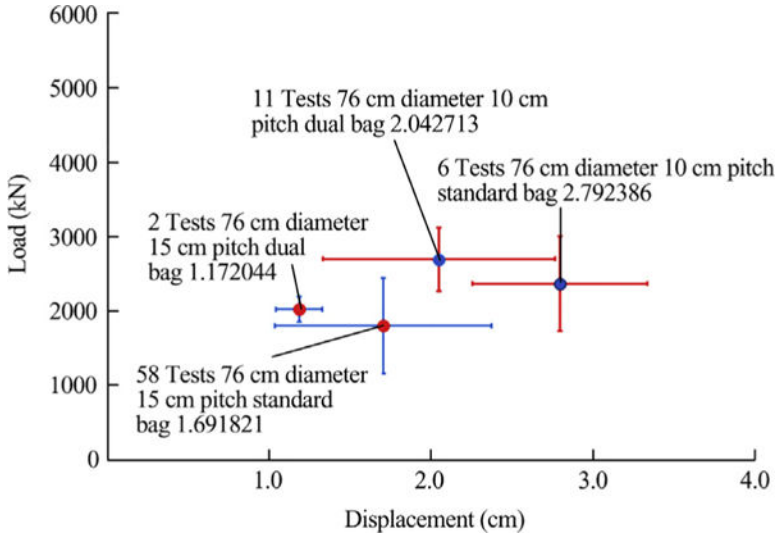

Fig. 21.

Comparison of the peak loading capacity of single-wall vs. dual-wall supports.

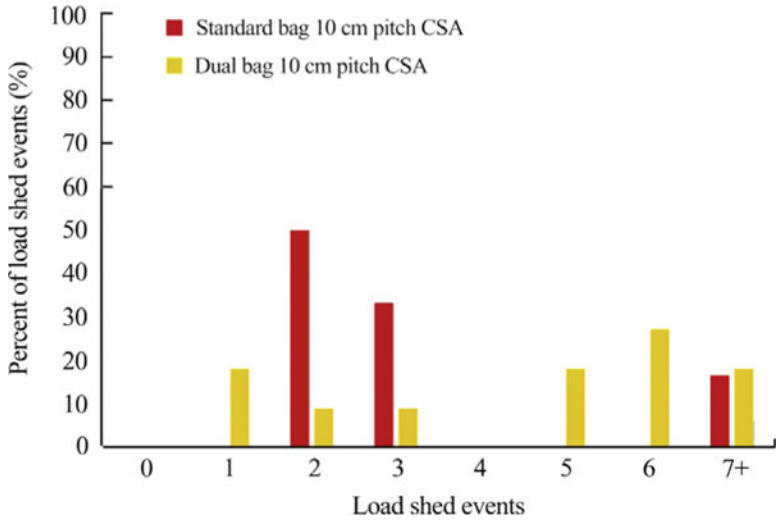

Fig. 22.

Distribution of the percentage of the number of load sheds occurring after the peak load capacity for single-wall and dual-wall pumpable roof supports.

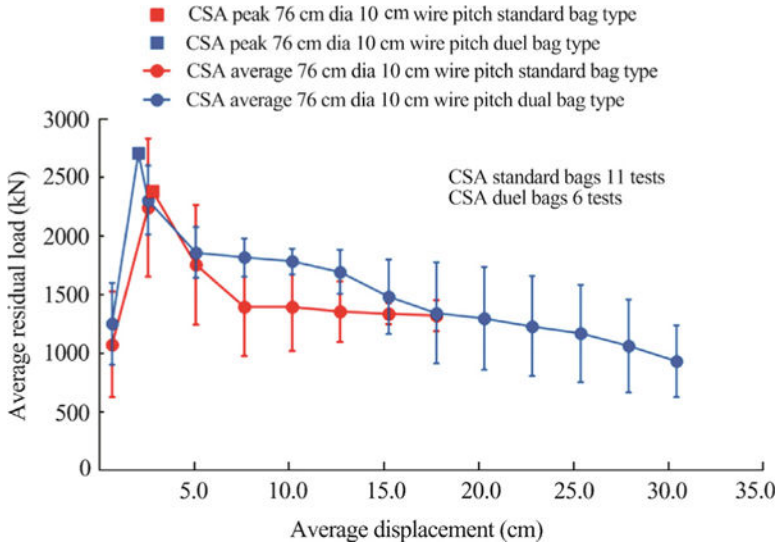

Fig. 23.

Representative average loading performance for single-wall and dual-wall pumpable roof supports.

Table 1

Comparison of support loading stiffness for CSA and Portland-based supports.

Diameter (cm)	Stiffness (kN/cm)	Peak load (kN)
(a) CSA-based material		
61	2250	1468
69	2270	1953
76	2338	2033
91	3888	3723
(b) Portland-based material		
61	904	1535
69	1114	1664
76	1228	1744
91	1308	2500

Table 2

Comparison of support loading stiffness for 7, 10, 15 cm wire spacing Portland-based supports.

Diameter (cm)	Wire pitch (cm)	Stiffness (kN/cm)	Peak load (kN)
69	8	1425	2108
69	10	1198	1548
69	15	883	1414

Table 3

Comparison of support loading stiffness for single-wall and dual-wall supports of CSA-based material.

Bag type	Diameter (cm)	Wire pitch (cm)	Stiffness (kN/cm)	Peak load (kN)
Single-wall	76	10	2317	2389
Dual-Wall	76	10	2718	2713
Single-wall	76	15	2196	1819
Dual-Wall	76	15	2949	2046